

Time-Dependent Three-Body Reactive Scattering in Hyperspherical Coordinates

Gregory A. Parker
Jeffery Crawford
Zachary Eldredge

Homer L. Dodge Department of Physics and Astronomy
University of Oklahoma

6 March 2013

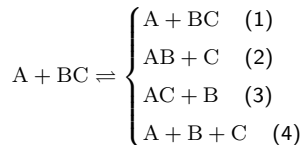


Outline

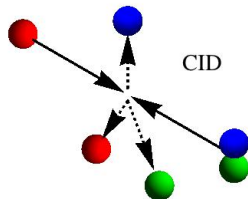
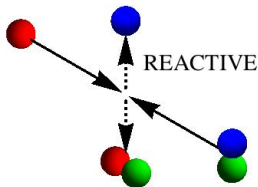
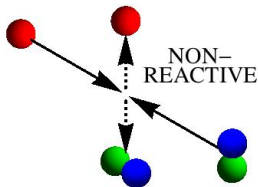
- Three-Body Quantum Reactive Scattering
- Applications
- Coordinates
 - Jacobi
 - APH
- Scattering Processes: 1D and 3D
- Scattering Methods:
 - Time-Independent
 - Time-Dependent
- Hyperspherical Time-Dependent Method
 - Initial wave packet
 - Evolution
 - Analysis
- Computational Efficiency
 - Symmetry
 - Sylvester-Like Algorithm
- Results

Three-Body Quantum Reactive Scattering

Interested in Reactions of the Form:



- Non-Reactive : (1)
 - Elastic
 - Inelastic
- Reactive : (2) and (3)
- Collision-Induced Dissociation : (4) or its time reversal Three-Body Recombination



Applications of Three-Body Collisions

- Ultra-Cold Atomic Systems
 - Three-body recombination leads to trap loss
 $A + B + C \rightarrow (ABC) \rightarrow A + BC$
 - Limits maximum density in Bose-Einstein Condensates
- Chemical Lasers
 $F + H_2 \rightarrow H + HF$
- Ozone Formation
- Positronium Formation
 $e^+ + H \rightarrow e^+e^- + p$
- Neutron detection: ${}^3\text{He}$, ${}^6\text{Li}$, ${}^{10}\text{B}$
 - $n + {}^3\text{He} \rightarrow {}^1\text{H} + {}^3\text{H}$
 - Rewritten as $n + {}^1\text{H}^2\text{H} \rightarrow {}^1\text{H} + {}^2\text{H}$
 $A + BC \rightarrow B + CA$

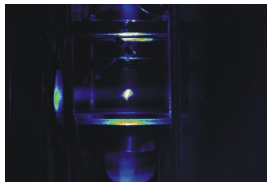


Figure : MOT Image (Courtesy of the Shaffer research group:
<http://www.nhn.ou.edu/~shaffer/research/ultracold.html>)



Figure : Chemical Laser (Courtesy of the Office of Naval
Research: <http://science.dodlive.mil/tag/lasers/>)

Coordinates

- System of 3 atoms: A, B, and C
- 3 Atoms \rightarrow 9 Coordinates
- Choose physically meaningful coordinate sets
- Relative Coordinates:
3 Internal + 3 Orientation + 3 Center-of-Mass

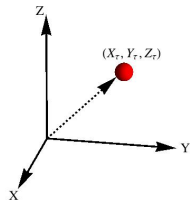


Figure : Space Fixed Axes

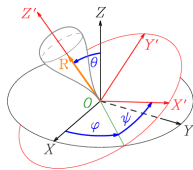
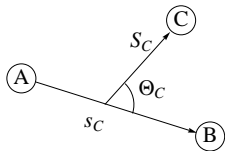
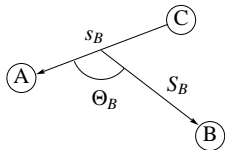
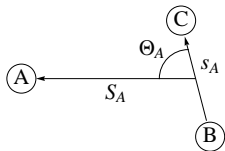


Figure : Euler Angles

Jacobi Coordinates

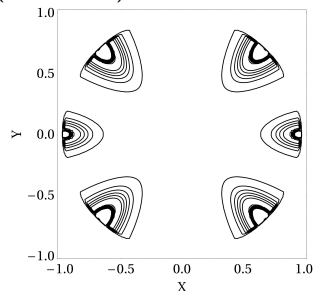
- Body-Fixed: $S_T, s_T, \Theta_T, \alpha_T, \beta_T, \gamma_T$
- Mass-scaled
- S_T : Reaction Coordinate
- s_T : Vibrational Coordinate
- Θ_T : Rotational Coordinate
- Appropriately describe $A + BC$ scattering states
- Single set does NOT treat each arrangement channel equivalently
- Not optimal for treating $A + B + C$ products: double continuum



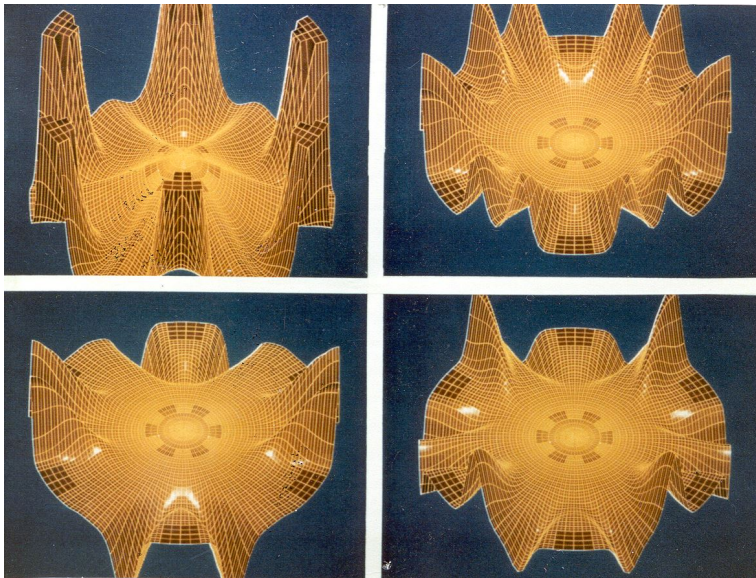
APH Coordinates

APH = Adiabatically Adjusting, Principal Axes Hyperspherical (Coordinates)

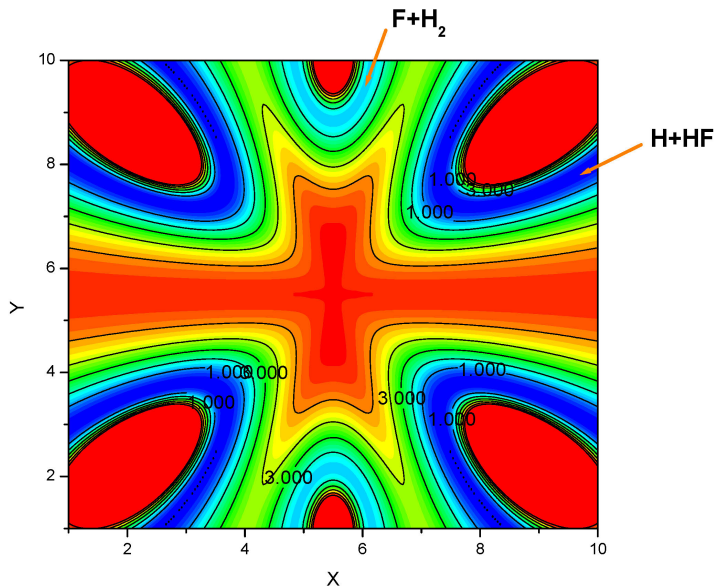
- Body Fixed: $\rho, \theta, \chi_i, \alpha_Q, \beta_Q, \gamma_Q$
- ρ : Size of three-body system
- θ : "Bending" angle: Collinear to equilateral triangle
- χ_i : Kinematic angle: $\frac{s_\tau}{S_\tau} \rightarrow 0$ as $\chi_\tau \rightarrow 0$
- Treats all arrangement channels equivalently
- Single continuum: Appropriate for $A + B + C$
- Covers configuration space twice



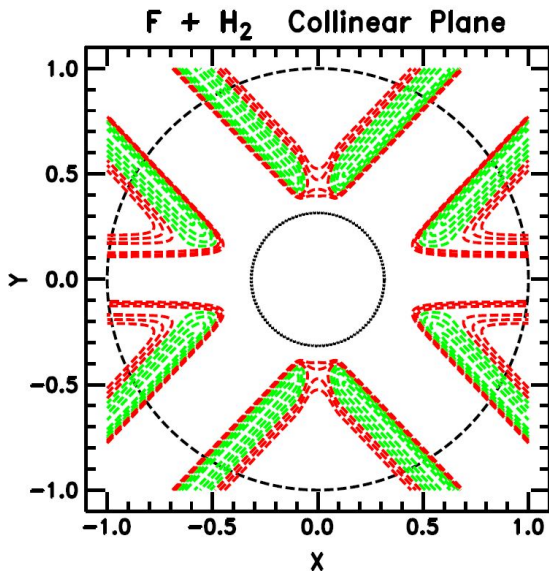
H₃ Potential and Surface Functions



F+H₂ Potential (Hyperspherical at constant ρ)

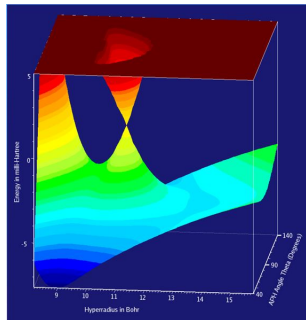
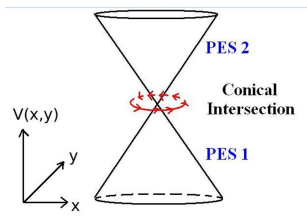


F+H₂ Potential (Collinear)



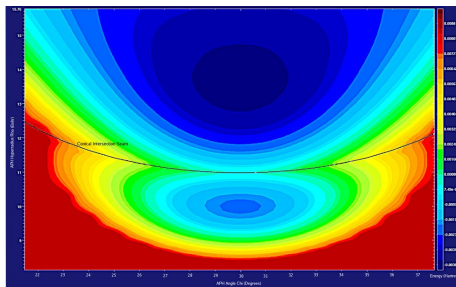
Geometric Phase

- Electronic potential energy surfaces (PESs) can cross to form conical intersections
- Berry (1984), Mead and Truhlar (1979) showed that, when a real electronic wavefunction moves on a closed loop which encircles the conical intersections, it needs to change sign.
- This change of sign effect is referred as the geometric phase effect
- This double-valuedness of the electronic wavefunction can have a non-trivial effect to the reactive scattering process
- Molecular AharonovBohm effect



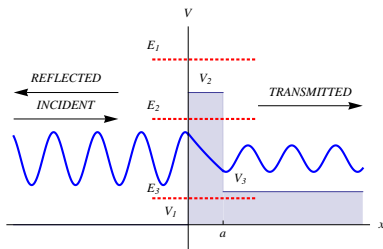
Spin-Aligned Triatomic Lithium

- Xuan Li derived the equations necessary to treat conical intersection that occur at collinear geometries
- Even at ultracold temperatures, the wavefunction is able to completely move around the conical intersections
- Non-trivial Geometric Phase effect
- Locations of conical intersections are not in a straight line in the internal coordinates
- Difficulties in using body-fixed internal coordinates



1D Scattering: Time-Independent

- Quantum mechanical treatment
- Single energy
- Two arrangement channels
- Only translation: kinetic energy
- Simple boundary conditions
- Wave functions must be well-defined over all space.



1D Scattering: Time-Dependent

1D Scattering

- Gaussian Envelope
- Initial-Value Problem
- Range of energies
- Two arrangement channels
- Match to TI boundary conditions only asymptotically

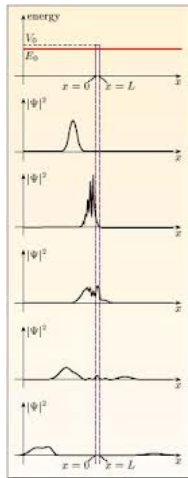
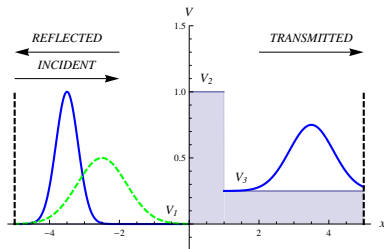
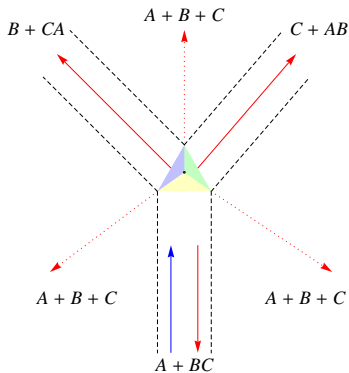
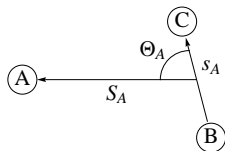


Figure : Wave Packet Evolution (Courtesy of LabSpace:
<http://labspace.open.ac.uk/mod/resource/view.php?id=347269>)

3D Scattering

- Three arrangement channels
- Energy stored in added degrees of freedom:
 - electronic
 - vibration
 - rotation
- Translational coordinate boundary conditions same as 1D case
- Vibrational-rotational boundary conditions: Match to basis functions



Time-Independent Methods

- Solve Time-Independent Schrödinger equation
- Calculates entire scattering matrix at a single energy:
All initial states \rightarrow All final states
- Accurate, efficient results
 - low energies
 - systems that support fewer bound states: H_3 , Li_3 , HNe_2
- Limited to time-independent Hamiltonians

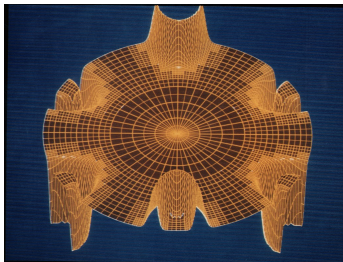
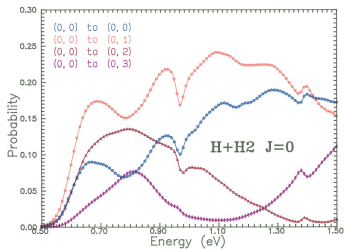


Figure : APH Surface Function: $\nu = 0, j = 0$

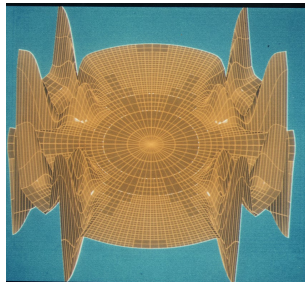


Figure : APH Surface Function: $\nu = 1, j = 2$

- Solve Time-Dependent Schrödinger equation (TDSE): Initial-Value Problem

$$i\hbar \frac{\partial}{\partial t} \varphi^{JM_p}(t) = \mathcal{H} \varphi^{JM_p}(t), \quad (1)$$

- Calculates a column of the scattering matrix for a range of energies:
A single initial state \rightarrow All final states
- More favorable computational scaling
- Initial-state does NOT have to be an eigenstate of the system
- Easier to locate energy-dependent scattering resonances
- Intuitive picture of scattering dynamics

Hyperspherical Time-Dependent Wave Packet Method

- 1 Construct the initial wave packet for state-to-state scattering
 - Use Jacobi coordinates for $A + BC$ reactants
 - Place in asymptotic region of potential energy surface at $t = 0$
- 2 Construct the initial wave packet for processes like photoassociation, photodissociation and coherent control
 - The initial wave packet is determined by the physical process and is often inside the interaction region at $t = 0$
- 3 Propagate the wave packet in time
 - Time evolution operator expressed in APH coordinates
 - Sample wave packet at a constant $\rho = \rho_\infty$ after each time step
- 4 Analyze wave packet
 - Project sampled wave packet onto APH surface functions
 - Fourier transform overlaps: Time \rightarrow Energy
 - Match to appropriate boundary conditions: S-matrix

The Initial Wave Packet

To get state-to-state S-matrix elements, construct an initial wave packet for A + BC:

$$\varphi_{\tau_i \nu_{ij} \ell_i}^{JM p}(t=0) = \frac{1}{s_{\tau_i} S_{\tau_i}} g_{\tau_i}(S_{\tau_i}) \mathcal{X}_{\tau_i \nu_{ij}}(s_{\tau_i}) \mathcal{Y}_{\tau_i j \ell_i}^{JM}(\hat{s}_{\tau_i}, \hat{S}_{\tau_i}). \quad (2)$$

Three terms of interest:

- $g_{\tau_i}(S_{\tau_i})$: Gaussian for reaction coordinate S_{τ_i}
- $\mathcal{X}_{\tau_i \nu_{ij}}(s_{\tau_i})$: Diatomic ro-vibrational eigenfunction for s_{τ_i}
- $\mathcal{Y}_{\tau_i j \ell_i}^{JM}(\hat{s}_{\tau_i}, \hat{S}_{\tau_i})$: Rotational eigenfunctions for Θ_{τ_i} , α_{τ_i} , β_{τ_i} , and γ_{τ_i}

$$\begin{aligned} \mathcal{Y}_{\tau_i j \ell_i}^{JM}(\hat{s}_{\tau_i}, \hat{S}_{\tau_i}) &= \left(\frac{2\ell_i + 1}{2J + 1} \right)^{1/2} \sum_{\Omega} C(j \ell_i J; \Omega 0 \Omega) \\ &\quad \times \hat{P}_{j\Omega}(\Theta_{\tau_i}) \hat{D}_{\Omega M}^J(\alpha_{\tau_i}, \beta_{\tau_i}, \gamma_{\tau_i}), \end{aligned} \quad (3)$$

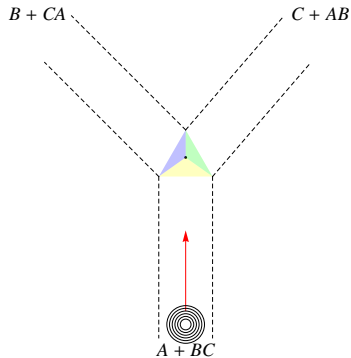
The Initial Wave Packet II

Place initial wave packet in asymptotic region

- Mapped to APH grid

$$\varphi_i^{J\Lambda p}(\rho, \theta, \chi_i, t=0) = \frac{\rho^{5/2}}{4} \int dQ \hat{D}_{\Lambda M}^{Jp*} \varphi_i^{JMp}(t=0) \quad (4)$$

- Momentum directed toward interaction region



Evolution of the Wave Packet

For time-independent Hamiltonian, propagate with time evolution operator:

$$\varphi^{JMP}(t) = e^{-i\mathcal{H}\Delta t/\hbar} \varphi^{JMP}(t=0). \quad (5)$$

Use Chebychev method:

$$e^{-i\mathcal{H}\Delta t/\hbar} \varphi^{JMP}(t=0) \approx e^{i(E_{max}-E_{min})\Delta t/2\hbar} \sum_{n=0}^{N_C} (2 - \delta_{n0}) i^n J_n(R) T_n(-i\bar{\mathcal{H}}) \varphi^{JMP}(t=0) \quad (6)$$

where

$$\bar{\mathcal{H}} = \frac{E_{max} + E_{min} - 2\mathcal{H}}{E_{max} - E_{min}} \quad (7)$$

$$R = \frac{1}{2\hbar} (E_{max} - E_{min}) \Delta t, \quad (8)$$

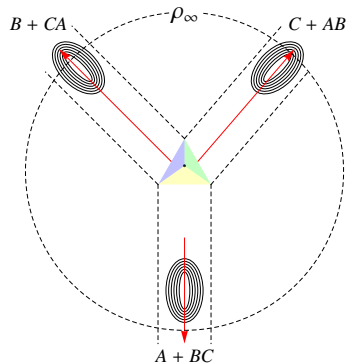
The terms in the sum are calculated using the Chebychev recursion relation

$$\Phi_n = -2i\bar{\mathcal{H}}\Phi_{n-1} - \Phi_{n-2}, \quad (9)$$

where $\Phi_n = T_n(\bar{\mathcal{H}}) \varphi^{JMP}(t=0)$.

Evolution of the Wave Packet II

- As time increases, the wave packet translates into interaction region
- Reflected or transmitted to asymptotic region
- Sample at ρ_∞ after each time step



TDWP

Analysis of the Wave Packet

- The wave packet can be expressed in terms of it's stationary state components at ρ_∞ :

$$\varphi_i^{J\Lambda p}(\rho_\infty, \theta, \chi_i, t) = \frac{1}{2\pi\hbar} \int_0^\infty dE e^{-iEt/\hbar} \eta_i(E) \Psi^{J\Lambda ip}(\rho_\infty) \quad (10)$$

- The energy eigenfunctions can be expanded as:

$$\Psi^{J\Lambda ip}(\rho_\infty) = - \sum_f S_{f,i}^J(E) \Psi_f^{J\Lambda ip}(E; \rho_\infty) \quad (11)$$

- Project both sides of Eq. (10) onto the APH surface functions:

$$F_{\kappa\Lambda,i}^J(t; \rho_\infty) = \frac{1}{2\pi\hbar} \int_0^\infty dE e^{-iEt/\hbar} \eta_i(E) \sum_f A_{\kappa\Lambda,f}^J(E; \rho_\infty) S_{f,i}^J(E) \quad (12)$$

- Fourier Transform Eq. (12) to extract S matrix elements from the integral

Analysis of the Wave Packet II

- After the Fourier transform:

$$\sum_f A_{\kappa\Lambda,f}^J(E; \rho_\infty) S_{f,i}^J(E) = F_{\kappa\Lambda,i}^J(E; \rho_\infty) \quad (13)$$

- The $F_{\kappa\Lambda,i}^J(E; \rho_\infty)$ are the Fourier transformed overlaps of the sampled wave packet with the APH surface functions:

$$F_{\kappa\Lambda,i}^J(E; \rho_\infty) = \frac{1}{\eta_i(E)} \int_0^\infty dt e^{iEt/\hbar} F_{\kappa\Lambda,i}^J(t; \rho_\infty) \quad (14)$$

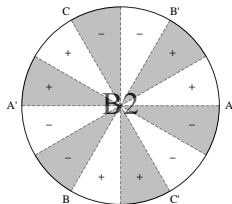
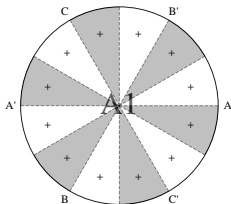
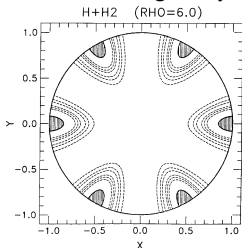
- The S matrix elements are obtained by solving the matrix equation:

$$\mathbf{A}^J \mathbf{S}^J = \mathbf{F}^J \quad (15)$$

Computation

To increase computational efficiency:

- Take advantage of symmetry of the potential energy surface

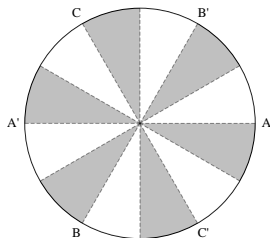
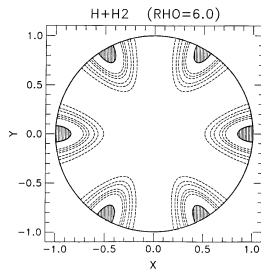


- Optimize most time-consuming portion of the program: Sylvester-like algorithm

$$(\mathbf{f}_\rho \otimes \mathbf{f}_\theta \otimes \mathbf{h}_\chi) \text{vec}(\Psi_t) = \begin{pmatrix} \text{vec}(\mathbf{Y}_\chi[:, 1, :]) \\ \text{vec}(\mathbf{Y}_\chi[:, 2, :]) \\ \vdots \\ \text{vec}(\mathbf{Y}_\chi[:, n_\rho, :]) \end{pmatrix} = \text{vec}(\mathbf{Y}_\chi) \quad (16)$$

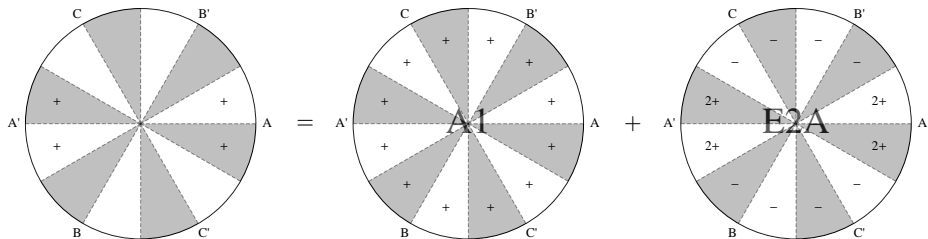
Symmetry: $H + H_2$

- Covers configuration space twice
- One unique arrangement: $H + H_2$
- Six reflection planes
- Three rotational symmetries
- Four 1D and two 2D irreducible representations
- Represent wave function on $1/12$ or $1/6$ of total space



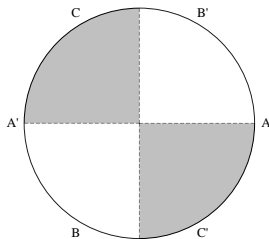
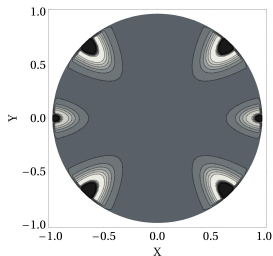
Symmetry: $H + H_2$

Express initial wave packet as a linear combination of irreducible representation wave packets.
 Consider a $\nu = 0, j = 0$ initial state:



Symmetry: $F + H_2$

- Two unique arrangements: $F + H_2$ and $H + HF$
- C_{2v} Symmetry
- Two reflection planes
- One rotational symmetry
- Represent wave function on 1/4 of the total space
- Four 1D irreducible representations



Symmetry: Implementation

- Propagate irreducible representation components of the initial wave packet:

$$\varphi_{\tau_i \nu_i j_i \ell_i}^{J\Lambda p \Gamma}(\theta, \chi_i, t = 0; \rho_\infty) = P^\Gamma \varphi_{\tau_i \nu_i j_i \ell_i}^{J\Lambda p}(\theta, \chi_i, t = 0; \rho_\infty) \quad (17)$$

- Expand in terms of energy eigenfunctions labeled by irreducible representation:

$$\varphi_i^{J\Lambda p \Gamma}(\rho_\infty, \theta, \chi_i, t) = \frac{1}{2\pi\hbar} \int_0^\infty dE e^{-iEt/\hbar} \eta_i(E) \Psi^{J\Lambda i \Gamma} \quad (18)$$

- Project onto surface functions belonging to the appropriate irreducible representation and Fourier transform:

$$\sum_{f'} A_{\kappa\Lambda, f'}^{J\Gamma}(E; \rho_\infty) S_{f', i}^{J\Gamma}(E) = F_{\kappa\Lambda, i}^{J\Gamma}(E; \rho_\infty) \quad (19)$$

- Arrangement channel dependent S matrix elements are obtained

$$S_{f, i}^J(E) = \sum_{\Gamma} \bar{P}_{ff'}^\Gamma S_{f', i}^{J\Gamma}(E) \quad (20)$$

$$\bar{P}_{ff'}^\Gamma = \langle \Psi_f^{J\Lambda i p} | \Psi_{f'}^{J\Lambda i \Gamma} \rangle \quad (21)$$

Sylvester-Like Algorithm

- Matrix-Vector Multiplication:

$$\mathbf{C}\mathbf{x} = (\mathbf{B} \otimes \mathbf{A})\text{vec}(\mathbf{X}) \quad (22)$$

- Sylvester Algorithm:

$$(\mathbf{B} \otimes \mathbf{A})\text{vec}(\mathbf{X}) = \text{vec}(\mathbf{A}\mathbf{X}\mathbf{B}^T) \quad (23)$$

- Can express the application of the APH Hamiltonian as a sum of Kronecker products:

$$H = -\frac{\hbar^2}{2\mu\rho^2} \frac{1}{\sin^2\theta} \frac{\partial^2}{\partial\chi^2} - \frac{\hbar^2}{2\mu\rho^2} \frac{4}{\sin 2\theta} \frac{\partial}{\partial\theta} \sin 2\theta \frac{\partial}{\partial\theta} - \frac{\hbar^2}{2\mu} \frac{\partial^2}{\partial\rho^2} + V \quad (24)$$

$$\mathbf{H}\psi_t = (\mathbf{f}_\rho \otimes \mathbf{f}_\theta \otimes \mathbf{h}_\chi + \mathbf{f}_\rho \otimes \mathbf{h}_\theta \otimes \mathbf{I}_\chi + \mathbf{h}_\rho \otimes \mathbf{I}_\theta \otimes \mathbf{I}_\chi + \mathbf{V})\text{vec}(\Psi_t) \quad (25)$$

- To reduce number of multiplications, each kinetic energy term can be expressed in a more efficient form:

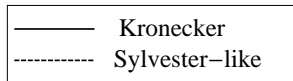
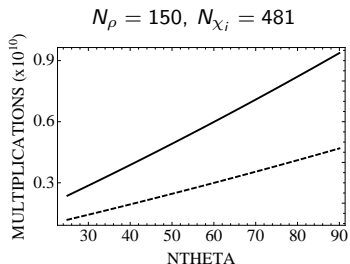
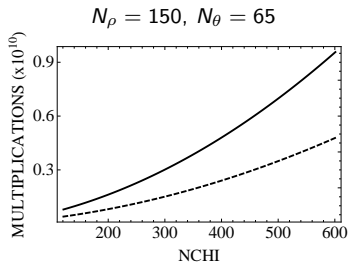
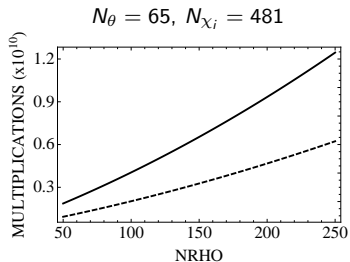
$$\mathbf{H}\psi_t = \text{vec}(\mathbf{Y}_\chi) + \text{vec}(\mathbf{Y}_\theta) + \text{vec}(\mathbf{Y}_\rho) + \mathbf{V}\text{vec}(\Psi_t) \quad (26)$$

$$\mathbf{Y}_\chi[:, j, k] = f_\rho[j, j] f_\theta[k, k] \mathbf{h}_\chi \Psi_t[:, j, k] \quad (27)$$

$$\mathbf{Y}_\theta[:, j, :] = f_\rho[j, j] \Psi_t[:, j, :] \mathbf{h}_\theta^T \quad (28)$$

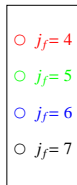
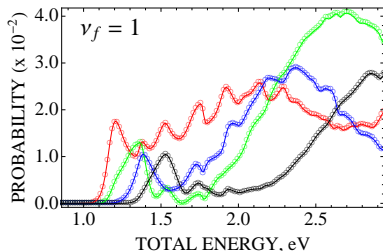
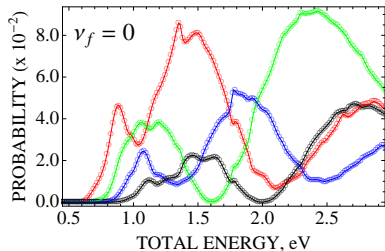
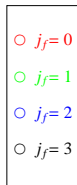
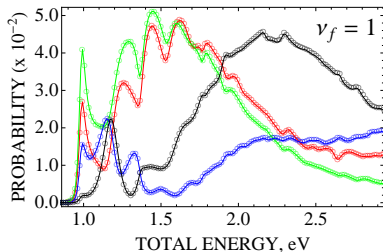
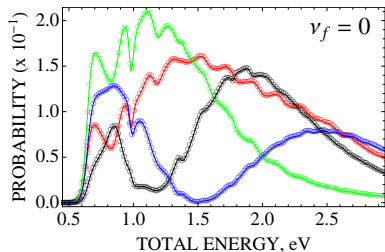
$$\mathbf{Y}_\rho[:, :, k] = \Psi_t[:, :, k] \mathbf{h}_\rho^T \quad (29)$$

Sylvester-Like Algorithm II



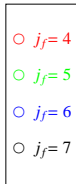
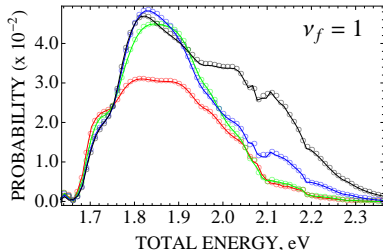
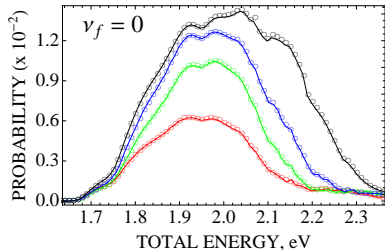
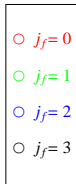
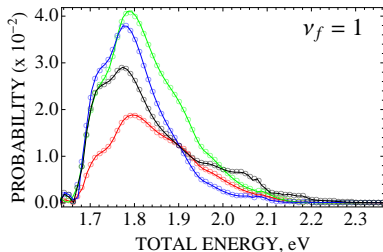
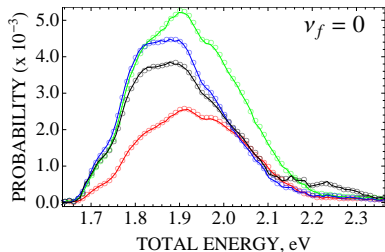
Number of multiplications required to apply the Hamiltonian to the wave packet.

Results: H + H₂



State-to-state reaction probabilities for $\text{H} + \text{H}_2(\nu_i = j_i = 0) \rightarrow \text{H}_2(\nu_f, j_f) + \text{H}$ on the DMBE potential energy surface.

Results: F + H₂



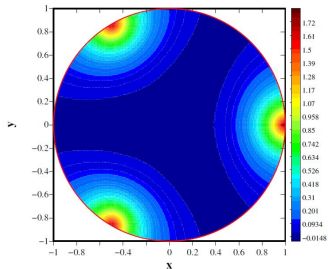
State-to-state reaction probabilities for $F + H_2(\nu_i = j_i = 0) \rightarrow HF(\nu_f, j_f) + H$ on the SW potential energy surface.

Conclusion

- Derived new hyperspherical, time-dependent method to extract three-body scattering information
- Derived Sylvester-like method to increase computational efficiency
- Obtained excellent agreement with TI benchmark results

Reviewer Quote:

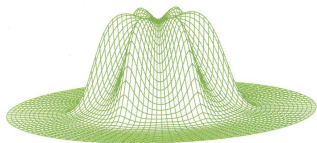
“Although hyperspherical wave packet calculations have been presented before, the present paper is leagues ahead in terms of the detail and clarity of the theory and the accuracy of the results.”



Future Work

Future Work:

- Implementation of non-uniform grids
- Time-Dependent Hamiltonians
- Inclusion of multiple electronic states
- Inclusion of Conical Intersections with vector potentials
- Inclusion of Conical Intersections with multiple electronic states
- Inclusion of magnetic, electric and electromagnetic fields
- Intense laser fields and the Floquet method
- Implement sensitivity analysis



Surface Function for H3

END

QUESTIONS?



The University of Oklahoma®

HOMER L. DODGE DEPARTMENT OF PHYSICS AND ASTRONOMY

$$T = -\frac{\hbar^2}{2\mu} \left(\frac{1}{S_\tau} \frac{\partial^2}{\partial S_\tau^2} S_\tau + \frac{1}{s_\tau} \frac{\partial^2}{\partial s_\tau^2} s_\tau \right) + \frac{\mathcal{L}_\tau^2}{2\mu S_\tau^2} + \frac{\mathcal{J}_\tau^2}{2\mu s_\tau^2} \quad (30)$$

$$\begin{aligned} T = & -\frac{\hbar^2}{2\mu\rho^{5/2}} \frac{\partial^2}{\partial \rho^2} \rho^{5/2} + \frac{15\hbar^2}{8\mu\rho^2} \\ & - \frac{\hbar^2}{2\mu\rho^2} \left[\frac{4}{\sin 2\theta} \frac{\partial}{\partial \theta} \sin 2\theta \frac{\partial}{\partial \theta} + \frac{1}{\sin^2 \theta} \frac{\partial^2}{\partial \chi_i^2} \right] \\ & + \frac{1}{\mu\rho^2} \left[\mathcal{A}_\theta J_x^2 + \mathcal{B}_\theta J_y^2 + \mathcal{C}_\theta J_z^2 - i\hbar \mathcal{D}_\theta J_y \frac{\partial}{\partial \chi_i} \right], \end{aligned} \quad (31)$$

$$\Psi^{JM_i} = \sum_{\tau\nu j\ell} \frac{1}{s_\tau S_\tau} G_{\tau\nu j\ell}^{J_i}(S_\tau) \mathcal{X}_{\tau\nu j}(s_\tau) \mathcal{Y}_{\tau j\ell}^{JM}(\hat{s}_\tau, \hat{S}_\tau). \quad (32)$$

$$\begin{aligned} \mathcal{Y}_{\tau j\ell}^{JM}(\hat{s}_\tau, \hat{S}_\tau) &= \left(\frac{2\ell + 1}{2J + 1} \right)^{1/2} \sum_{\Omega} C(j\ell J; \Omega 0 \Omega) \\ &\quad \times \hat{\mathcal{P}}_{j\Omega}(\Theta_\tau) \hat{D}_{\Omega M}^J(\alpha_\tau, \beta_\tau, \gamma_\tau), \end{aligned} \quad (33)$$

$$\begin{aligned}
 G_{\tau\nu j\ell}^{Ji}(S_\tau) &\xrightarrow{S_\tau \rightarrow \infty} \left(\frac{\mu}{2\pi\hbar^2 k_{\tau\nu j}} \right)^{1/2} \\
 &\times \left\{ \delta_{\tau\tau_i} \delta_{\nu\nu_i} \delta_{jj_i} \delta_{\ell\ell_i} e^{-i(k_{\tau\nu j} S_\tau - \ell\pi/2)} \right. \\
 &\left. - S_{\tau\nu j\ell, \tau_i\nu_i j_i \ell_i}^J(E) e^{i(k_{\tau\nu j} S_\tau - \ell\pi/2)} \right\}, \tag{34}
 \end{aligned}$$

$$\Psi^{JM_p} = \sum_{\kappa\Lambda} \frac{4}{\rho^{5/2}} \psi_{\kappa\Lambda}^{J_p}(\rho) \Phi_{\kappa\Lambda}^{J_p}(\theta, \chi_i; \rho_\xi) \hat{D}_{\Lambda M}^{J_p}(\alpha_Q, \beta_Q, \gamma_Q), \quad (35)$$

$$\left\{ -\frac{\hbar^2}{2\mu\rho_\xi^2} \left[\frac{4}{\sin 2\theta} \frac{\partial}{\partial\theta} \sin 2\theta \frac{\partial}{\partial\theta} + \frac{1}{\sin^2\theta} \frac{\partial^2}{\partial\chi^2} \right] + \frac{15\hbar^2}{8\mu\rho_\xi^2} \right. \\ \left. + \frac{1}{\mu\rho^2} \left[\frac{\mathcal{A}_\theta + \mathcal{B}_\theta}{2} \hbar^2 J(J+1) + \left(\mathcal{C}_\theta - \frac{\mathcal{A}_\theta + \mathcal{B}_\theta}{2} \right) \hbar^2 \Lambda^2 \right] \right. \\ \left. + V(\theta, \chi_i; \rho_\xi) - \mathcal{E}_{\kappa\Lambda}^{J_p} \right\} \Phi_{\kappa\Lambda}^{J_p}(\theta, \chi_i; \rho_\xi) = 0, \quad (36)$$

$$\begin{aligned}
 \varphi_{\tau_i \nu_i j_i \ell_i}^{JM}(\mathbf{t} = 0) &= \frac{1}{s_{\tau_i} S_{\tau_i}} g_{\tau_i}(S_{\tau_i}) \mathcal{X}_{\tau_i \nu_i j_i}(s_{\tau_i}) \\
 &\times \left(\frac{2\ell + 1}{2J + 1} \right)^{1/2} \sum_{\Omega} C(j \ell J; \Omega 0 \Omega) \\
 &\times \hat{\mathcal{P}}_{j_i \Omega_i}(\Theta_{\tau_i}) \hat{D}_{\Omega_i M}^J(\alpha_{\tau_i}, \beta_{\tau_i}, \gamma_{\tau_i}).
 \end{aligned} \tag{37}$$

$$g_{\tau_i}(S_{\tau_i}) = \left(\frac{1}{2\pi\sigma^2} \right)^{1/4} e^{-(S_{\tau_i} - S_{\tau_i}^0)^2 / 4\sigma^2} e^{-ik_0 S_{\tau_i}}. \tag{38}$$

$$\mathcal{H}\varphi^{J\Lambda p}(\rho, \theta, \chi_i, t) \quad (39)$$

$$\begin{aligned} & \left\{ -\frac{\hbar^2}{2\mu} \frac{\partial^2}{\partial \rho^2} + \frac{15\hbar^2}{8\mu\rho^2} - \frac{\hbar^2}{2\mu\rho^2} \left[\frac{4}{\sin 2\theta} \frac{\partial}{\partial \theta} \sin 2\theta \frac{\partial}{\partial \theta} + \frac{1}{\sin^2 \theta} \frac{\partial^2}{\partial \chi_i^2} \right] \right\} \varphi^{J\Lambda p}(\rho, \theta, \chi_i, t) \\ & + \left\{ V(\rho, \theta, \chi_i) + \frac{1}{\mu\rho^2} \left[\frac{\mathcal{A}_\theta + \mathcal{B}_\theta}{2} \hbar^2 J(J+1) + \left(\mathcal{C}_\theta - \frac{\mathcal{A}_\theta + \mathcal{B}_\theta}{2} \right) \Lambda^2 \right] \right\} \varphi^{J\Lambda p}(\rho, \theta, \chi_i, t) \\ & - \frac{1}{\mu\rho^2} \sum_{\Lambda'=0}^J \left\langle \hat{D}_{\Lambda M}^{Jp} \left| \frac{\mathcal{A}_\theta - \mathcal{B}_\theta}{2} (J_x^2 - J_y^2) - i\hbar \mathcal{D}_\theta J_y \frac{\partial}{\partial \chi_i} \right| \hat{D}_{\Lambda' M}^{Jp} \right\rangle \varphi^{J\Lambda' p}(\rho, \theta, \chi_i, t), \quad (40) \end{aligned}$$